ACS Photonics

Article

pubs.acs.org/journal/apchd5

Electrodynamic Modeling of Quantum Dot Luminescence in Plasmonic Metamaterials

Ming Fang,*,†,‡ Zhixiang Huang,*,† Thomas Koschny,‡ and Costas M. Soukoulis‡,§

†Key Laboratory of Intelligent Computing and Signal Processing, Ministry of Education, Anhui University, Hefei 230001, China

‡Ames Laboratory and Department of Physics and Astronomy, Iowa State University, Ames, Iowa 50011, United States

§Institute of Electronic Structure and Laser, FORTH, 71110 Heraklion, Crete, Greece

ABSTRACT: A self-consistent approach is proposed to simulate a coupled system of quantum dots (QDs) and metallic metamaterials. Using a four-level atomic system, an artificial source is introduced to simulate the spontaneous emission process in the QDs. We numerically show that the metamaterials can lead to multifold enhancement and spectral narrowing of photoluminescence from QDs. These results are consistent with recent experimental studies. The proposed method represents an essential step for developing and understanding a metamaterial system with gain medium inclusions.

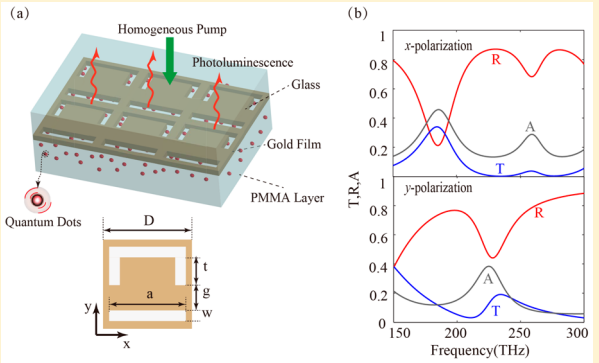

KEYWORDS: *photoluminescence, plasmonics, metamaterials, quantum dots, finite-different time-domain, spontaneous emission*

The fields of plasmonic metamaterials have made spectacular experimental progress in recent years.[1−3] The metal-based metamaterial losses at optical frequencies are unavoidable. Therefore, control of conductor losses is a key challenge in the development of metamaterial technologies. These losses hamper the development of optical cloaking devices and negative index media. Recently, several theoretical[4−7] and experimental[8−19] studies demonstrated that one promising way to reduce or even compensate for the losses is through combining the metamaterial with a gain medium. The experimentally realized gain materials include organic semiconductor quantum dots (QDs),[15] quantum wells,[18] and dyes.[20] These studies mainly focused on the coupling between the gain media and the metamaterial. Without the coupling system, no loss compensation can occur, and the transmitted signal cannot be amplified. In addition, this method can be used to obtain new nanoplasmonic lasers by incorporating gain in the metamaterial.[21−23] Improving the laser gain material and developing a lasing spaser device constitute a significant target of this research. An essential part of this development is the study of luminescence of gain media embedded into metamaterials. Understanding the mechanism underlying the coupling between the metamaterial and the gain media when these materials are combined is highly important.

Active optical devices, which are used in such applications as spasers, laser cooling of atoms, amplifiers, quantum computing, plasmons, and enhanced spontaneous emission in microcavity plasmons, require a detailed understanding of the interaction between electromagnetic fields and quantum physics-based gain materials. This requirement has generated increased interest in device design based on quantum electrodynamics. In an active medium, the electromagnetic field is treated classically, whereas atoms are treated quantum mechanically. According to the current understanding, the interaction of electromagnetic fields with an active medium can be modeled by a classical harmonic oscillator model and the rate equations of atomic population densities.[24] Thus, simulations of lasing and amplification in active devices are simple. For example, the finite-difference time-domain (FDTD) method is frequently used to study the temporal quantum electrodynamics of active systems. In fact, this method has been used to investigate compensation, amplification, and lasing behaviors in various active systems.[25−27]

However, numerical simulation of spontaneous emission cannot be directly implemented using this method because in the numerical experiments we can simulate the loss compensation and lasing dynamics in active systems using a probe source, such as a Gaussian pulse. To simulate spontaneous emission, we should provide a suitable source for the coherent FDTD iteration. There are some promising methods to numerically calculate spontaneous emission.[28−31] Here, we present a systematic time-domain simulation of the quantum electrodynamic behavior of an active metamaterial system. An artificial source placed in a gain medium associated with the local population inversion is proposed as the probe source in the numerical experiment. We investigate the loss compensation and emission enhancement in a system of QDs

Received: September 7, 2015
Published: March 18, 2016

DOI: 10.1021/acsphotonics.5b00499
ACS Photonics 2016, 3, 558−563

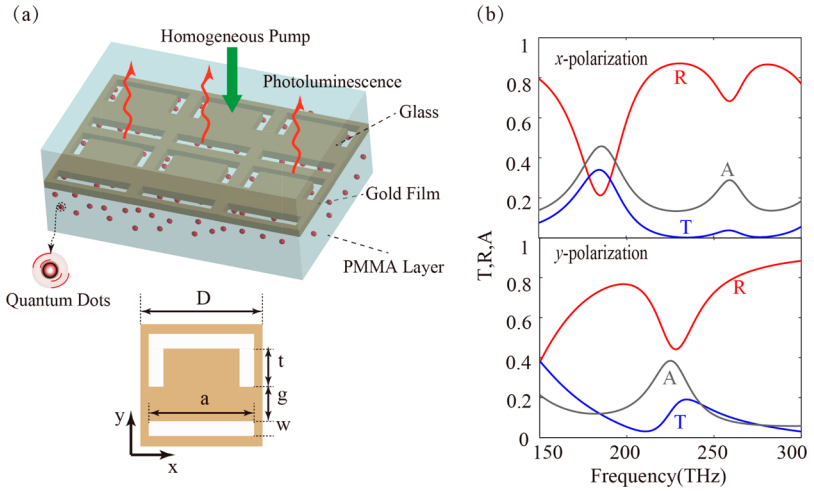

Figure 1. (a) Schematic of a metamaterial functionalized with QDs. (b) Calculated transmittance T, reflectance R, and absorptance A spectra for the coupled system shown in (a) with a unit cell size of 545 nm. The metamaterial feature sizes are D = 545 nm, lateral slit a = 470 nm, top vertical slit and gap $t = g$ = 170 nm, and slit width w = 65 nm.

coupled to a metamaterial, considering both the resonant spectra of the metamaterial and the pumping power. The numerical simulation results demonstrate that QDs' photoluminescence properties can be greatly enhanced and regulated by the metamaterial. This result represents an important step in the development and understanding of active metamaterial devices.

THEORETICAL MODEL FOR THE NUMERICAL EXPERIMENTS

Maxwell's equations in the time domain for an isotropic media are given by

$$\nabla \times \mathbf{E}(\mathbf{r}, t) = -\partial \mathbf{B}(\mathbf{r}, t)/\partial t,\ \nabla \times \mathbf{H}(\mathbf{r}, t) = \partial \mathbf{D}(\mathbf{r}, t)/\partial t \tag{1}$$

where $\mathbf{B}(\mathbf{r}, t) = \mu\mu_0\mathbf{H}(\mathbf{r}, t)$, and $\mathbf{D}(\mathbf{r}, t) = \varepsilon\varepsilon_0\mathbf{E}(\mathbf{r}, t) + \mathbf{P}(\mathbf{r}, t)$. Additionally, $\mathbf{P}(\mathbf{r}, t) = \mathbf{P}[\mathbf{E}]$ is the dynamic polarization response, and $\mathbf{P}(\mathbf{r}, t) = \mathbf{P}[\mathbf{E}]$ has a nonlinear functional dependence on the local electric field. In the frequency domain, $\mathbf{P}(\omega) = \varepsilon_0\chi(\omega)\ \mathbf{E}(\omega)$ is associated with a number of fundamental electronic response models. We model the metallic metamaterial and active medium using the Drude and Lorentz models, respectively.

In the numerical experiments, gain medium is described by a generic four-level system, and electrons are pumped by a homogeneous pumping rate f_{pump} from the ground state level (N_0) to the third level (N_3). After a short lifetime τ_{32}, electrons nonradiatively relax into the upper emission level (N_2). When electrons radiatively transfer from upper emission energy to lower emission level, they radiate photons at the central frequency $\omega_e = (E_2 - E_1)/\hbar$. Lastly, electrons transfer quickly and nonradiatively from the first level to the ground-state level. The atomic population densities obey the following rate equations:

$$\begin{aligned}
\frac{\partial N_3(r,t)}{\partial t} &= f_{pump}N_0(r,t) - \frac{N_3(r,t)}{\tau_{32}},\\
\frac{\partial N_2(r,t)}{\partial t} &= \frac{N_3(r,t)}{\tau_{32}} + \frac{1}{\hbar\omega_e}\mathbf{E}(r,t)\cdot\frac{\partial \mathbf{P}(r,t)}{\partial t} - \frac{N_2(r,t)}{\tau_{21}},\\
\frac{\partial N_1(r,t)}{\partial t} &= \frac{N_2(r,t)}{\tau_{21}} - \frac{1}{\hbar\omega_e}\mathbf{E}(r,t)\cdot\frac{\partial \mathbf{P}(r,t)}{\partial t} - \frac{N_1(r,t)}{\tau_{10}},\\
\frac{\partial N_0(r,t)}{\partial t} &= \frac{N_1(r,t)}{\tau_{10}} - f_{pump}N_0(r,t)
\end{aligned} \tag{2}$$

where f_{pump} is the homogeneous pumping rate.[32] In order to solve the response of the active materials in the electromagnetic fields numerically, the auxiliary differential equation (ADE) FDTD method is utilized.[33,34] This method enables us describe the dynamic electronic responses as induced polarization currents in both linear and nonlinear regimes. For the purpose of saving computing time and storage space, the initial condition of the four-level system is set as the saturated state; that is, the population number changes very slowly with time. By the initial condition, we do not need a pump process and a long time decay for pump pulse. The population numbers at each level can be obtained as

$$\begin{aligned}
N_0 &= N_{tot}/((\tau_{10} + \tau_{21} + \tau_{32})f_{pump} + 1),\\
N_1 &= N_{tot}\tau_{10}f_{pump}/((\tau_{10} + \tau_{21} + \tau_{32})f_{pump} + 1),\\
N_2 &= N_{tot}\tau_{21}f_{pump}/((\tau_{10} + \tau_{21} + \tau_{32})f_{pump} + 1),\\
N_3 &= N_{tot}\tau_{32}f_{pump}/((\tau_{10} + \tau_{21} + \tau_{32})f_{pump} + 1)
\end{aligned} \tag{3}$$

The spontaneous emission in an active medium originates from the radiative process between the upper emission level and lower emission level. Here an artificial source is introduced to numerically simulate the spontaneous emission. We assume all electrons in the upper level radiatively transit to lower

DOI: 10.1021/acsphotonics.5b00499
ACS Photonics 2016, 3, 558−563

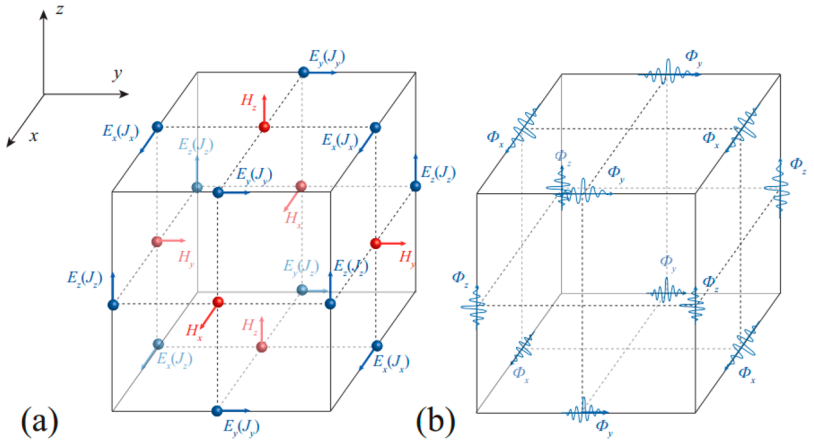

Figure 2. Diagram of the artificial dipoles in the Yee cell. Each dipole has its own direction and random phase.

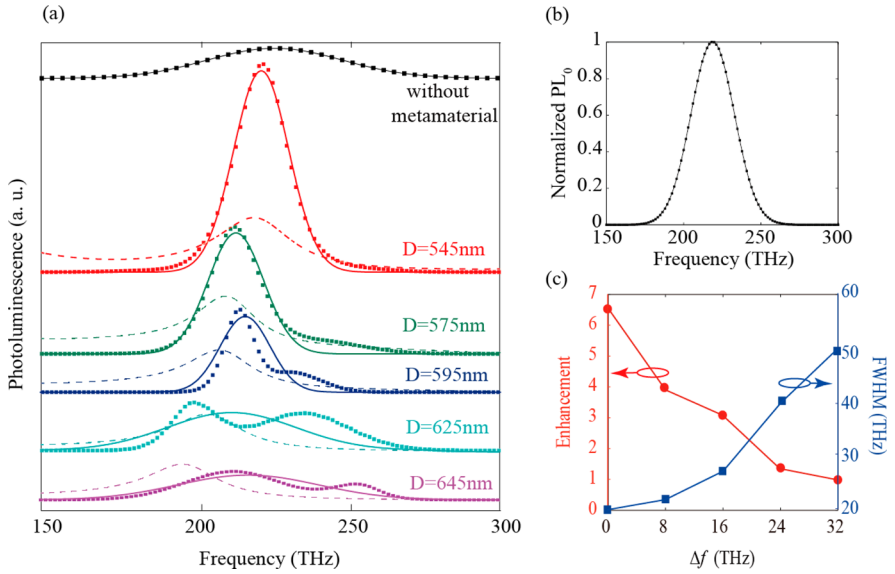

Figure 3. (a) Photoluminescence of the QDs without (black line, PL_0) and with different unit size metamaterials (dotted lines, 545 to 645 nm) with a pumping rate of 17×10^8 s^{-1}. The dashed lines indicate the metamaterial's absorption spectra, and the solid lines are the Gaussian fits of the dotted lines. (b) Profile of the photoluminescence spectrum without a metamaterial layer. (c) Intensity enhancement and fwhm of the QD−metamaterial coupled device's photoluminescence spectra. The enhancement is normalized to the photoluminescence peak intensity without the metamaterial (PL_0).

emission level. The effect on the electric field of a spontaneously emitted photon is accounted for by scaling the number of excited electrons N_2 by the energy per photon at the emission frequency $\hbar\omega_e$. Thus, the amplitude of the artificial dipole source can be obtained by $\sqrt{N_2\hbar\omega_e\eta_0}$. Here η_0 is the wave impedance in the free space. The artificial dipole generates the probe source with the Lorentzian radiant spectrum, which is consistent with that of the gain material. We convert the spontaneous emission into a temporal pulse centered at time t_0. The temporal signal is desired because this allows us to perform a Fourier transform to study the spectral response. The field components are nodally uncollocated, as shown in Figure 2a. Such an arrangement of nodal quantities is naturally compatible with the rotational nature of the curl operator in the ADE-FDTD algorithm. For artificial source Φ, the nodal arrangement is shown in Figure 2b. To create a coupled system, the two separate grids are conjoined, such that (Φ_x, J_x, E_x), (Φ_y, J_y, E_y), and (Φ_z, J_z, E_z) are nodally collocated; the H components are uncollocated. Every artificial source is associated with each grid in the gain medium region. The phase of every artificial dipole has an individual random phase φ_{rand}. Within the ADE-FDTD simulation, spontaneous emission is introduced as an artificial dipole source in the electric field at a given mesh point:

$$\Phi(r_k, t) = \sqrt{N_2(r_k, t)\hbar\omega_e\eta_0}\ e^{-\pi((t-t_0)^2\Delta f)^2} \sin(\omega_e t + \varphi_{rand}) \quad (4)$$

Here, Δf is the frequency line width of the QDs, and k represents the x, y, and z coordinates. The amplitude of the artificial source is clearly dependent on the density of emission level N_2.

PHOTOLUMINESCENCE IN AN ACTIVE METAMATERIAL

We consider an iSRR array sandwiched between a glass substrate and a gain substrate with a square periodicity of D = 545 nm. The iSRR is made of gold, and its permittivity is characterized by a Drude model: $\varepsilon(\omega) = \varepsilon_\infty - \omega_p^2/(\omega^2 + i\omega\gamma)$,

DOI: 10.1021/acsphotonics.5b00499
ACS Photonics 2016, 3, 558−563

with $\varepsilon_\infty = 9$, $\omega_p = 2\pi \times 2.184 \times 10^{15}$ rad/s, and $\gamma = 2\pi \times 4.07 \times 10^{14}$ rad/s. The gain substrate consists of lead sulfide (PbS) semiconductor QDs. These QDs are dispersed in poly(methyl methacrylate) (PMMA), and the thickness of the QDs/PMMA substrate is 180 nm. The dielectric constant of the gain substrate is $\varepsilon_g = 2.2$, which corresponds to an average between QDs and PMMA. The 400 nm glass substrate is on top of the iSRR with dielectric constant $\varepsilon_s = 2.56$. In the following simulations, we set the emission frequency of the QDs as $\omega_e = 2\pi \times 223 \times 10^{12}$ rad/s, the line width as $\Gamma_a = 35 \times 10^{12}$ THz, and the coupling strength as $\sigma_a = 10^{-4}$ C^2/kg. The lifetime of each energy level is chosen to be $\tau_{32} = 0.05$ ps, $\tau_{21} = 80$ ps, and $\tau_{10} = 0.05$ ps.[21] The total electron density is $N_{tot} = N_0(t) + N_1(t) + N_2(t) + N_3(t) = 5.0 \times 10^{23}/m^3$.

We start the simulations by the initial condition as presented in the previous section. We use the artificial dipole source as a probe source. To calculate the photoluminescence, multiple monitors located above the glass substrate are used to record the electric field. Here, the monitors record the electric field in the y direction, along which the iSRR's Fano mode can be excited.[35] Eventually, an averaged result photoluminescence spectrum can be observed. To study the effect of the metamaterial's resonance of the photoluminescence spectrum, we use five samples with different unit cell sizes ranging from 545 to 645 nm. The photoluminescence of the QDs coupled with the metamaterial is presented in Figure 3a. All of the photoluminescence spectra are normalized to the photoluminescence peak intensity without a metamaterial layer. The dotted lines are the calculated photoluminescence spectra, and the solid lines indicate the Gaussian fits of the dotted lines. For $D = 545$ nm, the iSRR's resonance frequency matches the QD emission frequency. The photoluminescence intensity peak is enhanced by a factor of 6.4 with a pumping rate of 17×10^8 s^{-1}. (In this simulation, we assume that the PMMA/QDs layer is pumped by a strong plane wave. With the parameters we used here, the equivalent pump power is $I_{pump} = 2.59$ W/mm^2.) Meanwhile, compared to the photoluminescence without metamaterials, the full width at half-maximum (fwhm) is decreased to 24 THz from 35 THz. When the iSRR resonance is red-shifted by increasing the unit cell size D from 545 nm to 645 nm, the photoluminescence spectrum becomes weaker and broader. The photoluminescence spectrum under the PMMA/QDs layer has the same properties. However, the coupled strength of the metamaterial and QDs is inhomogeneous in the PMMA layer; this will lead to a slightly different photoluminescence spectrum shape from the photoluminescence spectrum up the glass substrate.

To further clarify the influence on the photoluminescence exerted by the coupling between the QDs and metamaterials, the photoluminescence enhancement and fwhm are shown as a function of Δf in Figure 4c. This figure indicates that the coupling between the emission of the QDs and the metamaterial is sensitive to the mismatch Δf. When the iSRR's resonance frequency is mismatched with the QD emission frequency, the photoluminescence peak is shifted from the QD emission frequency toward the respective iSRR's resonant frequency. For the larger mismatches at $D = 625$ nm and $D = 645$ nm, the photoluminescence spectrum becomes even broader than it is without the metamaterial and appears to develop two peaks close to the emission frequency and iSRR's resonant frequency.

In addition, we have investigated the relationship between the photoluminescence spectrum and the polarization state of the metamaterial. The metamaterials studied here have profound polarization-dependent properties. While a plasmonic Fano resonance is excited by the y-polarized external fields, this resonance vanishes for the x-polarized wave (see Figure 1b). This polarization dependence may be expected to affect the interaction with the QDs, and hence the polarization dependence of the photoluminescence was calculated, as illustrated by Figure 4, for the metamaterial with $D = 545$ nm. By changing the polarization from the y to the x direction, the absorption spectrum becomes featureless around f_0 (Figure 4b). The corresponding photoluminescence drastically degrades (Figure 4a), providing additional evidence that the photoluminescence spectrum is controlled by the plasmonic resonance.

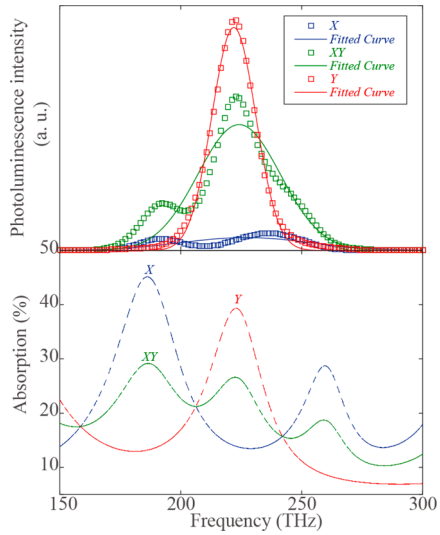

Figure 4. Polarization dependence of (a) photoluminescence and (b) absorption, measured for the metamaterial with $D = 545$ nm. Linear polarizations x and y are introduced in Figure 1b, while xy is the intermediate polarization at 45° to x.

One might attempt to explain such spectral shift and polarization dependence as a result of filtering the photoluminescence spectrum of QDs through the metamaterial. The metamaterials can be considered as a filter for the QDs' photoluminescence. By definition the power radiated from the QD as photons through photoluminescence, $PL(\omega)$, is simply proportional the photoluminescence quantum yield, $PL_0(\omega)$, of the absorbed power, $A(\omega)$, that is re-emitted radiatively. Hence, the photoluminescence is given by $PL(\omega) = PL_0(\omega) \times A(\omega)$. Here in our case, $A(\omega)$ is the absorption spectrum of the metamaterial and $PL_0(\omega)$ is the photoluminescence spectrum without the metamaterial. The solid-colored lines in Figure 5f illustrate the predicted photoluminescence using the formula $PL(\omega) = PL_0(\omega) \times A(\omega)$. The dashed lines indicate the absorption spectra of the metamaterial, and the solid black line is the photoluminescence of QDs without the metamaterial. The presence of the plasmonic metamaterial drastically changes the QD photoluminescence characteristics. Indeed, when the metamaterial resonance is red-shifted, the photoluminescence spectrum is weakened, broadened, and distorted. In all cases, the photoluminescence peak is shifted from its original position f_e toward the respective metamaterial's absorption resonance f_a. For the largest mismatch (i.e., solid purple line), the photoluminescence spectrum becomes non-Gaussian and appears to develop two peaks near the QD's emission

DOI: 10.1021/acsphotonics.5b00499
ACS Photonics 2016, 3, 558−563

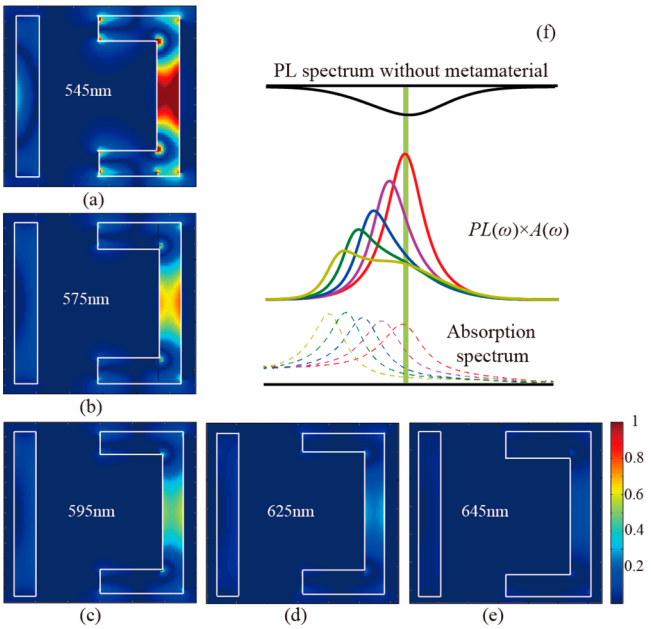

Figure 5. (a–e) Illustration of the metamaterials' electric field distribution with differently sized unit cells at each individual resonant frequency with a pumping rate of 17×10^8 s^{-1}. (f) The dashed lines indicate the absorption spectra of the metamaterial with different unit cell sizes, the solid black line denotes the photoluminescence of the QDs without the metamaterial, and the solid colored lines represent the predicted photoluminescence spectra.

frequency and the metamaterial's resonance, respectively. These predicted results are similar to the numerical results and exhibit the same change tendency. We calculated the electric field amplitude distribution in the cross-section of the iSRR layer (*xy* plane in Figure 1a). The detailed results are plotted in Figures 5a–e. When the metamaterial resonance is red-shifted, the electric fields in the iSRR cavity get weakened.

However, the previous explanation does not explain the observed photoluminescence enhancement resulting from the presence of the metamaterial. In order to explain the photoluminescence enhancement, we investigate the photoluminescence enhancement for different pumping rates with the matched case ($\Delta f = 0$, $D = 545$ nm). Figure 6a shows the calculated photoluminescence spectrum as a function of the pumping rate. The photoluminescence spectra in Figure 6a are normalized to the photoluminescence peak intensity without the metamaterial at the corresponding pumping rate. We find the photoluminescence enhancement is sensitive to the pumping rate. Indeed, the photoluminescence spectrum enhancement is proportional to the density of photon states that the photonic environment offers for spontaneous emission decay. Here we calculate the absorption of the coupled system. Figure 6b plots the absorption, with and without QDs. Without QDs, the absorption around resonance is broad and the fwhm is 41.2 THz. With the introduction of QDs under a pumping rate $f_{pump} = 17 \times 10^8$ s^{-1}, the resonance becomes narrower, and the fwhm reduces to a smaller value of 9.4 THz. So the coupled system creates a photonic environment equivalent to a nanocavity with a varying *Q*-factor and a mode volume that can be roughly calculated by $V = 2(a + t)\omega h$; that is, the mode volume is approximately equal to the slit volume. The enhancement of the *Q*-factor enhances the density of photon states, leading to the Purcell factor enhancement of photoluminescence: $F_p = \frac{3}{4\pi^2}\left(\frac{\lambda}{n}\right)^3 \frac{Q}{V}$,[36,37] from 69 without pumping rate to 296 with a pumping rate of 17×10^8 s^{-1}. Here, λ is the wavelength and n is the refractive index. Thus, the observed photoluminescence enhancement can be understood in terms of the enhancement of the Purcell factor. Figure 6c shows the photoluminescence enhancement of the photoluminescence spectra and *Q*-factor enhancement as a function of the pumping rate. The increasing pumping rate leads to a larger intensity enhancement factor and a higher *Q*-factor.

In conclusion, we have studied photoluminescence in QDs coupled to metamaterials by a time domain self-consistent approach. We have used a four-level atomic system for the modeling of QDs. An artificial source is introduced to simulate the spontaneous emission in the QDs. It is observed that a strong enhancement in photoluminescence occurs when the emission frequency of the QD lies near the metamaterial resonance frequencies. Our artificial source also can be used in three-level atomic systems. The present study can be used to make new types of optical devices for sensing, low-threshold lasing devices, and switching applications.

AUTHOR INFORMATION

Corresponding Authors

*E-mail: ahu_mingfang@yahoo.com.
*E-mail: zxhuang@ahu.edu.cn.

Notes

The authors declare no competing financial interest.

ACKNOWLEDGMENTS

Work at Ames Laboratory was partially supported by the U.S. Department of Energy (Basic Energy Sciences, Division of

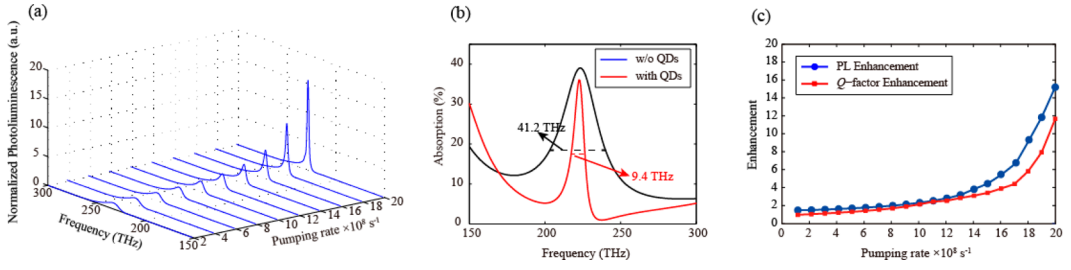

Figure 6. (a) QD–metamaterial photoluminescence spectra for different pump powers, normalized to the photoluminescence peak intensity without the metamaterial at the corresponding pumping rate. The unit size of the iSRR is set as $D = 545$ nm. (b) Absorption spectrum of metamaterial without and with QDs. (c) Plot of intensity enhancement and fwhm of the photoluminescence spectrum as a function of the pumping rate. These data are all normalized to the photoluminescence without the metamaterial.

DOI: 10.1021/acsphotonics.5b00499
ACS Photonics 2016, 3, 558–563

Materials Sciences and Engineering) under Contract No. DE-AC02-07CH11358. This work was supported by the National Natural Science Foundation of China under Grant Nos. 61101064, 51277001, 51477039, 61201122, NCET (NCET-12-0596) of China and DFMEC (No. 20123401110009), European Research Council under the ERC Advanced Grant No. 320081 (PHOTOMETA), and Anhui Provincial Natural Science Foundation (Nos. 1508085JD03, 1508185QF130).

REFERENCES

(1) Soukoulis, C. M.; Linden, S.; Wegener, M. Negative refractive index at optical wavelengths. *Science* **2007**, *315*, 47−49.
(2) Soukoulis, C. M.; Wegener, M. Optical metamaterials - more bulky and less lossy. *Science* **2010**, *330*, 1633−1634.
(3) Soukoulis, C. M.; Wegener, M. Past achievements and future challenges in the development of 3D photonic metamaterials. *Nat. Photonics* **2011**, *5*, 523−530.
(4) Moitra, P.; Yang, Y.; Anderson, Z.; Kravchenko, I. I.; Briggs, D. P.; Valentine, J. Realization of an all-dielectric zero-index optical metamaterial. *Nat. Photonics* **2013**, *7*, 791−795.
(5) Fang, A.; Huang, Z.; Koschny, Th.; Soukoulis, C. M. Overcoming the losses of a split ring resonator array with gain. *Opt. Express* **2011**, *19*, 12688−12699.
(6) Fang, A.; Koschny, Th.; Soukoulis, C. M. Self-consistent calculations of loss-compensated fishnet metamaterials. *Phys. Rev. B: Condens. Matter Mater. Phys.* **2010**, *82*, 121102.
(7) Sivan, Y.; Xiao, S.; Chettiar, K.; Kidishev, V.; Shalaev, V. M. Frequency-domain simulations of a negative-index material with embedded gain. *Opt. Express* **2009**, *17*, 24060−24074.
(8) Staude, I.; Khardikov, V. V.; Fofang, N. T.; Liu, S.; Decker, M.; Neshev, D. N.; Luk, T. S.; Brener, I.; Kivshar, Y. S. Shaping photoluminescence spectra with magnetoelectric resonances in all-dielectric nanoparticles. *ACS Photonics* **2015**, *2*, 172−177.
(9) Campione, S.; Albani, M.; Capolino, F. Complex modes and near-zero permittivity in 3D arrays of plasmonic nanoshells: loss compensation using gain. *Opt. Mater. Express* **2011**, *1*, 1077−1089.
(10) Wuestner, S.; Pusch, A.; Tsakmakidis, K.; Hamm, M.; Hess, O. Overcoming losses with gain in a negative refractive index metamaterial. *Phys. Rev. Lett.* **2010**, *105*, 127401.
(11) Gordon, J. A.; Ziolkowski, R. W. CNP optical metamaterials. *Opt. Express* **2008**, *16*, 6692−6716.
(12) De Luca, A.; Bartolino, R.; Correa-Duarte, A.; Curri, M. L.; Steinmetz, N. F.; Strangi, G. Gain-assisted plasmonic metamaterials: mimicking nature to go across scales. *Rendiconti Lincei* **2015**, *26*, 161−174.
(13) Infusino, M.; De Luca, A.; Veltri, A.; Vazquez-Vazquez, C.; Correa-Duarte, M. A.; Dhama, R.; Strangi, G. Loss mitigated collective resonances in gain-assisted plasmonic mesocapsules. *ACS Photonics* **2014**, *1*, 371−376.
(14) Lepetit, T.; Akmansoy, Es.; Ganne, J. P. Experimental measurement of negative index in an all-dielectric metamaterial. *Appl. Phys. Lett.* **2009**, *104*, 121101.
(15) Plum, E.; Fedotov, A.; Kuo, P.; Tsai, P.; Zheludev, I. Towards the lasing spaser: controlling metamaterial optical response with semiconductor quantum dots. *Opt. Express* **2009**, *17*, 8548−8551.
(16) Tanaka, K.; Plum, E.; Ou, Y.; Uchino, T.; Zheludev, N. I. Multifold enhancement of quantum dot luminescence in plasmonic metamaterials. *Phys. Rev. Lett.* **2010**, *105*, 227403.
(17) Geng, J.; Ziolkowski, R. W.; Jin, R.; Liang, X. Active cylindrical coated nano-particle antennas: polarization dependent scattering properties. *J. Electromag. Waves Appl.* **2013**, *27*, 1392−1406.
(18) Meinzer, N.; Ruther, M.; Linden, S.; Soukoulis, C. M.; Khitrova, G.; Hendrickson, J.; Olitzky, D.; Gibbs, M.; Wegener, M. Arrays of Ag split-ring resonators coupled to InGaAs single-quantum-well gain. *Opt. Express* **2010**, *18*, 24140−24151.
(19) Xiao, S.; Drachev, P.; Kildishev, V.; Ni, X.; Chettiar, K.; Yuan, K.; Shalaev, V. M. Loss-free and active optical negative index metamaterials. *Nature* **2010**, *466*, 735−738.
(20) Meinzer, N.; Konig, M.; Ruther, M.; Linden, S.; Khitrova, G.; Gibbs, M.; Busch, K.; Wegener, M. Distance-dependence of the coupling between split-ring resonators and single-quantum-well gain. *Appl. Phys. Lett.* **2011**, *99*, 111104.
(21) Oulton, F.; Sorger, J.; Zentgraf, T.; Ma, M.; Gladden, C.; Dai, L.; Bartal, G.; Zhang, X. Plasmon lasers at deep subwavelength scale. *Nature* **2009**, *461*, 629−632.
(22) Noginov, A.; Zhu, G.; Belgrave, M.; Bakker, R.; Shalaev, V. M.; Narimanov, E.; Stout, S.; Herz, E.; Suteewong, T.; Wiesner, U. Demonstration of a spaser-based nanolaser. *Nature* **2009**, *460*, 1110−1112.
(23) Stockman, I. Spasers explained. *Nat. Photonics* **2008**, *2*, 327−329.
(24) Huang, Z.; Koschny, Th.; Soukoulis, C. M. Theory of pump-probe experiments of metallic metamaterials coupled to a gain medium. *Phys. Rev. Lett.* **2012**, *108*, 187402.
(25) Nagra, S.; York, A. FDTD analysis of wave propagation in nonlinear absorbing and gain media. *IEEE Trans. Antennas Propag.* **1998**, *46*, 334−340.
(26) Zhou, J.; Koschny, Th.; Soukoulis, C. M. An efficient way to reduce losses of left-handed metamaterials. *Opt. Express* **2008**, *16*, 11147−11152.
(27) Fang, A.; Koschny, Th.; Soukoulis, C. M. Lasing in metamaterial nanostructures. *J. Opt.* **2009**, *12*, 024013.
(28) Valentine, J.; Zhang, S.; Zentgraf, T.; Ulin-Avila, E.; Genov, A.; Bartal, G.; Zhang, X. Three-dimensional optical metamaterial with a negative refractive index. *Nature* **2006**, *445*, 376−379.
(29) Pusch, A.; Wuestner, S.; Hamm, J. M.; Tsakmakidis, K. L.; Hess, O. Coherent amplification and noise in gainenhanced nanoplasmonic metamaterials: a Maxwell-Bloch Langevin approach. *ACS Nano* **2009**, *6*, 2420−2431.
(30) Slavcheva, G. M.; Arnold, J. M.; Ziolkowski, R. W. FDTD Simulation of the Nonlinear Gain Dynamics in Active Optical Waveguides and Semiconductor Microcavities. *IEEE J. Sel. Top. Quantum Electron.* **2004**, *10*, 1052−1062.
(31) Decker, M.; Decker, M.; Staude, I.; Shishkin, I. I.; Samusev, K. B.; Parkinson, P.; Sreenivasan, V. K. A.; Minovich, A.; Miroshnichenko, A. E.; Zvyagin, A.; Jagadish, C.; Neshev, D. N.; Kivshar, Y. S. Dual-channel spontaneous emission of quantum dots in magnetic metamaterils. *Nat. Commun.* **2013**, *4*, 2949.
(32) For a thin gain slab illuminated by a plane wave the pumping rate is equivalent to the pump intensity. The pump power density is equal to $\hbar\omega_e f_{pump} N_0$, and the pump intensity I_{pump} = (pump power)/(surface area) = $\hbar\omega_e f_{pump} N_0$(volume)/(surface area) = $\hbar\omega_e f_{pump} N_0 d$; here d is the thickness of the gain slab.
(33) Taflove, A.; Hagness, C. *Computational Electrodynamics: The Finite-Difference Time Domain Method*; Artech House: Norwood, MA 2005.
(34) Wuestner, S.; Pusch, A.; Tsakmakidis, K.; Hamm, M.; Hess, O. Gain and plasmon dynamics in active negativeindex metamaterials. *Philos. Trans. R. Soc., A* **2011**, *369*, 3525−3550.
(35) Lukyanchuk, B.; Zheludev, N. I.; Maier, S. A.; Halas, N. J.; Nordlander, P.; Giessen, H.; Chong, C. T. The Fano resonance in plasmonic nanostructures and metamaterials. *Nat. Mater.* **2010**, *9*, 707−715.
(36) Novotny, L.; Hecht, B. *Principles of Nano-optics*; Cambridge University Press, 2006.
(37) Vahala, K. *Optical Microcavities*; World Scientific Publishing Company, 2004.

DOI: 10.1021/acsphotonics.5b00499
ACS Photonics 2016, 3, 558−563